REACTION OF MANGANESE CONTAINING SLAG WITH CARBON SUBSTRATE

H. Sun[1,2], M. Lone[1], S. Ganguly[3] and O. Ostrovski[1]

[1] School of Material Science and Engineering, University of New South Wales, Sydney, NSW 2052, Australia; h.sun@unsw.edu.au; o.ostrovski@unsw.edu.au
[2] Steel and Aluminum R&D Department, China Steel Corp., Kaohsiung, Taiwan 81233, ROC
[3] Hatch, 61 Petrie Terrace, Brisbane, Australia; sganguly@hatch.com.au

ABSTRACT

Reduction of MnO from slag and wetting of carbonaceous materials were studied in reaction of synthetic and industrial ferromanganese slags with graphite and coke substrates by the sessile drop method at 1450 - 1550 °C. Reduced metal was found at slag-substrate interface and at gas-slag-substrate boundary of slag perimeter. The reduced metal was mainly manganese with small amount of dissolved silicon and carbon. The reduction rate of MnO increased with increasing activity of MnO in slag and temperature. The rate of MnO reduction from industrial slag was faster than from the synthetic slag; slag was more reactive with a coke substrate than with a graphite substrate. The reduction rate was observed to increase with increasing ash content in the substrate. The dynamic contact angle between a carbon substrate and slag varied in a range of 80° to 140° and decreased in the process of reaction. A lower contact angle was observed for a substrate with a higher ash content.

1 INTRODUCTION

The reactions between carbonaceous materials and molten slag during the carbothermal reduction of manganese ore are key reactions in production of manganese alloys. There are still significant gaps in understanding of mechanisms of MnO reduction [1]. The kinetics of reduction of manganese ore and factors affecting the ore reduction have been intensively studied [2-10]. Rankin and Van Danverter [2], and Rankin and Wynnyckyj [3] suggested two possible mechanisms for the reduction of manganese oxide; they are indirect reduction *via* gas phase and direct reduction at the interfaces of slag-coke or slag-reduced alloy. These studies showed that the rate of the overall MnO reduction is limited by the Boudouard reaction [2], or by transport of CO_2 from the gas-slag interface to the gas-carbon interface [3]. Ostrovski and Webb [4] investigated the reduction of high siliceous manganese ore by graphite at 900-1400 ºC. The reduction of manganese oxide was predominantly observed at the metal/slag interface by carbon in the metal phase.

It has been shown in a study of wettability of graphite by slag containing iron oxide [11,12], that the carbon-iron oxide reaction has a profound effect on the contact angle and interfacial tension between the carbon and slag. A comprehensive understanding of the reduction kinetics should include interfacial properties which affect carbon-slag contact area and gas bubbles formation at the reaction sites.

To further explore the mechanisms of MnO reduction, the reduction rate of MnO in slag by carbonaceous materials was investigated in this study using industrial multicomponent slag and synthetic quaternary slag, four different carbonaceous materials, and carbonaceous materials with different surface roughness over temperature range of 1450-1550 º C. The wettability between slag and carbon substrate during the reaction was also monitored.

2 EXPERIMENTAL

The experiments were conducted in a graphite furnace which schematic is presented in Figure 1.The study was based upon in-situ observation of high-temperature wettability of a solid substrate by molten slag using the sessile drop method. In these experiments, the change in behavior of a liquid drop of slag upon a graphite or coke substrate with time and temperature was recorded.

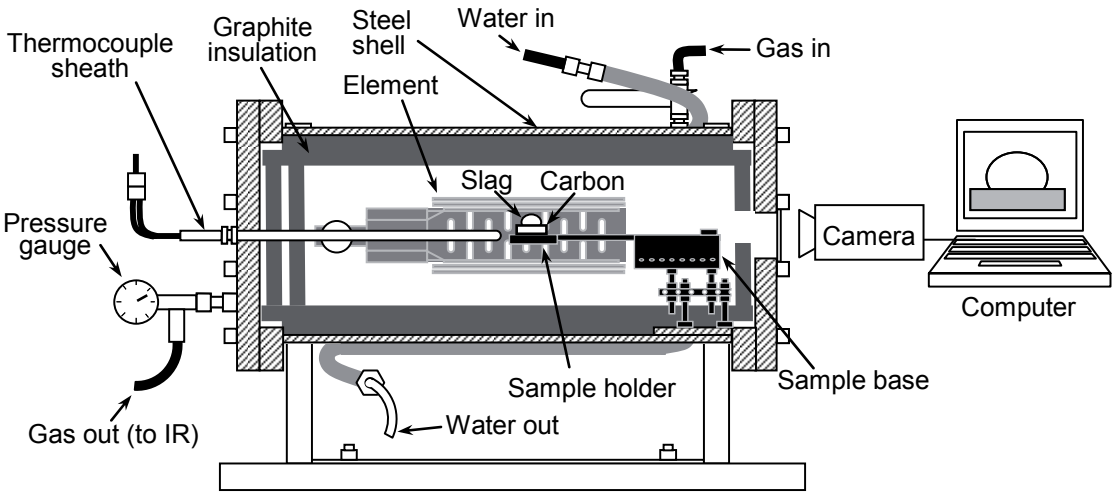

Figure 1: Experimental set-up.

A digital video camera with a resolution of 720×576 pixels was used to record image sequences during the wettability experiments. Zoom lenses (one 4×, one 1×) were added to the camera lens to provide the correct focal length. Welding lenses were placed in between the camera and the furnace window to reduce glare from the sample at high temperatures. The atmosphere in the reactor was maintained inert by passing purified argon with a flow rate of 1 L/min. The graphite furnace used in these experiments had very low thermal inertia; it had a potential to heat up a sample at a rate of more than 8 °C/s. The furnace was equipped with the circulation of cooling water, what provided the high cooling rate, particularly at temperatures >800 °C. This on one hand, excluded slag-substrate reaction in the process of heating and, on other hand, quenched a sample after completion of the experiment.

A solid slag sample was mounted on the top of the substrate and was preheated to the temperature close to but below the slag fusion temperature. Then the temperature was quickly increased to the experimental temperature to melt the slag what initiated carbon-slag reaction. The time required for melting slag was less than one minute. The moment when slag was fully melted was taken as a start of the reaction. After a certain reaction period, power was switched off, slag solidified within several seconds; and after cooling to the room temperature, samples were taken for the analysis. The variation of the slag composition with reaction time was determined from chemical analysis (XRF) of reacted slag samples. The reaction time was 1-3 hours. An IR gas analyser was used for measurement of the off gas composition.

Table 1: Composition of slag samples.

Slag	MnO	SiO_2	CaO	Al_2O_3	MgO	Na_2O	Fe
				mass%			
Synthetic							
A	37.3	33.4	18.4	9.6			
B	18.6	43.6	23.8	12.6			
C	13.9	46.1	25.3	13.4			
Industrial							
D	42.7	24.6	12.6	11.4	2.23	0.54	0.60
E	37.5	26.2	13.9	12.2	1.58	0.49	0.49
F	10.2	42.5	17.9	16.2	5.85		0.32

The reacted carbon substrate and slag samples were quite fragile. To protect them from mechanical damage during sample handling, the reacted substrate and slag were mounted in resin for cross-sectioning. The mounted samples were cut in half for analysis of the reacted interface between substrate and slag. The cross sectional surface of the slag-substrate interface was subjected to optical microscope, SEM and EDS analyses.

Chemical composition of synthetic and industrial slags is given in Table 1. Synthetic slags A, B and C are represented by the quaternary MnO-SiO_2-CaO-Al_2O_3 system. Preparation of these slags included melting a mixture of SiO_2, CaO and Al_2O_3 in a muffle furnace, its quenching, crushing, grounding and mixing with MnO. The mixture of all four oxides was sintered in an induction furnace with a graphite susceptor under argon for 1 hour at 1000 °C. The sinter was then ground and pressed into 0.6×10^{-3} kg tablets which were used in experiments. CaO:SiO_2:Al_2O_3 ratio of quaternary slag was targeted at 4:2:1, and MnO concentration varied from 13 to 40 mass%. Industrial slags D, E and F are represented by the MnO-SiO_2-CaO-Al_2O_3-MgO-Na_2O multicomponent system; it also contained a small amount of iron. The initial slag sample mass was 0.6×10^{-3} kg in all runs. Experimental observations and calculations using FACTSage (version 6.0 with a database developed by Tang and Olsen [13]) showed that all slags were molten at a temperature above 1250 °C.

Table 2: Composition of carbon substrates, mass%.

Carbon	Fixed Carbon	Ash	S	Ash Composition							
				SiO_2	Al_2O_3	CaO	MgO	TiO_2	Na_2O	K_2O	Fe
Coke 1	87.6	11.4	0.38	56.8	31.5	2.3	0.5	1.4	0.34	0.72	3.6
Coke 2	86.3	12.4	0.66								
Coke 3	84.1	13.6	0.34	50.2	35	4.2	1	1.4	0.55	0.65	4.5
Graphite	>99.5	<0.2									

The substrates were prepared from coke and graphite. They were cut into plates with a dimension of 10mm×10mm×2mm followed by surface progressive grinding. To study the effect of substrate surface finishing on reaction rate and on interfacial properties, several graphite substrates were filed using an 8 inch flat bastard file to increase the surface roughness while other substrates were polished by 1200 emery paper in running water and afterwards dewatering. Chemical analysis of substrates is given in Table 2. A major difference in the substrate chemistry was ash content and composition.

Table 3: MnO and SiO_2 activities in initial slags (a_{MnO}, a_{SiO2}), MnO reduction rates (*Rate*), apparent reduction rate constants (k) and average carbon-slag contact angles (θ).

Run	Slag	Carbon	a_{MnO}	a_{SiO_2}	*Rate*	k	θ
					mass%/h	mass%/h	°
1	A	Graphite	0.154	0.0931	0.36	2.34	126.5
2	A	Coke 1	0.154	0.0931	3.60	23.4	116.5
3	A	Coke 2	0.154	0.0931	5.10	33.1	120.5
4	A	Coke 3	0.154	0.0931	5.28	34.4	114.5
5	D	Coke 1	0.276	0.0273	9.72	35.2	110
6	D	Coke 2	0.276	0.0273	8.10	29.3	109.5
7	D	Coke 3	0.276	0.0273	10.2	37.0	97
8	D	Graphite	0.276	0.0273	4.38	15.9	119.5
9	B	Graphite	0.0345	0.255	0.18	5.57	129
10	C	Graphite	0.0211	0.293	0.012	0.57	134
11	E	Graphite	0.195	0.0461	2.16	11.0	110.5
12	F	Graphite	0.0127	0.299	0.66	50.6	112
13	A	RSG[*2]	0.154	0.0931	0.42	2.81	129
14[*1]	A	Graphite	0.131	0.0860	0	0	129

*1: Experimental temperature is 1450 ℃ for run 14 and 1550 ℃ for others.
*2: RSG means rough surface graphite.

3 RESULTS AND DISCUSSION

3.1 Visual Observations

The experimental conditions and results are summarised in Table 3. The images of the substrate-slag drop assembly before the reaction, at the experimental temperature in the run 1 and after the reaction at room temperature are presented in Figure 2. Once the slag was fully melted at the experimental temperature, it formed a liquid drop on the substrate seen in Figure 2(b). After the experiment, as seen in Figure 2(c) where the slag was set on the top of the substrate and in Figure 2(d) where the slag drop was taken off the substrate side, metal drops were found at the interface between slag and substrate and at the gas-slag-substrate boundary at slag perimeter. The reduced metal drop sandwiched at slag-substrate interface was further investigated using back scattered electron image of the interface of reacted sample in run 8, which studied reaction of slag D with graphite. The interface image is shown in Figure 3. Figure 3 also shows that the slag-metal interface was sharp while the substrate-metal interface appeared zigzag where many small carbon particles were cocooned in the metal matrix.

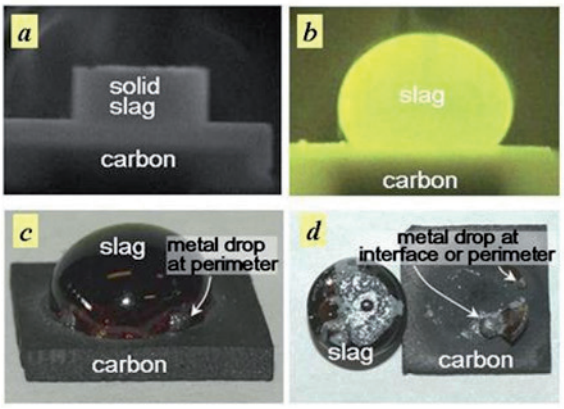

Figure 2: Appearance of slag and carbon substrate during heating (a), 7 minutes after heating to 1550 ℃ (b), after reaction (c) and reacted surfaces of slag and substrate (d) for run 1.

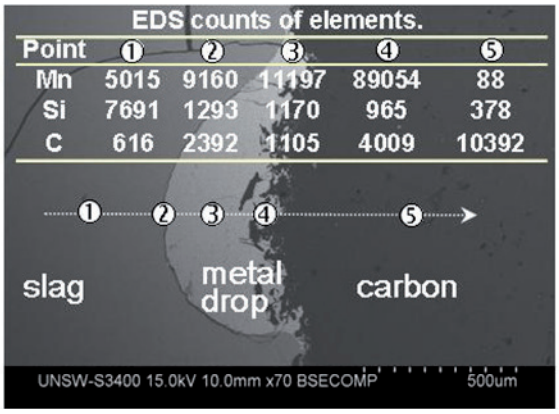

Figure 3: Cross sectional view of slag-carbon interface, metal drop at the interface and EDS analysis for run 8.

Table 4: Atomic ratio of concentration of elements to calcium in the slag bulk phase and in the vicinity of interface for run 8.

Element	EDS count at point 1	Atomic ratio	
		Bulk	Interface
Ca	3985	1	1
Si	7691	1.82	1.93
Al	3942	0.99	0.99
Mg	918	0.24	0.23
Mn	5015	2.67	1.26

3.2 Element Distribution at the Interface

The EDS spectrum along the dotted line in Figure 3 from the slag phase, across the slag-metal interface into the metal phase, and then across the metal-substrate interface into the substrate characterises relative manganese, silicon and carbon contents as a number of counts, which are summarised in the table in Figure 3. In the metal phase, formed in the reduction process, manganese was a major component, the Mn/Si and Mn/C atomic ratios in the metal were near 10:1 (9.6 and 10.1 correspondingly, point 3, Figure 3). This means that silicon and carbon were in the solution in

manganese. The number of counts for manganese, silicon, aluminium, calcium and magnesium at point 1 in Figure 3 is summarised in Table 4. The atomic ratio of the elements to calcium in slag was used to show the variation of slag composition. Calcium was chosen as a reference element in slag because CaO in slag is not involved in the reaction. The atomic ratios for the slag bulk phase were obtained from the composition of slag D given in Table 1. The atomic ratios of slag 2.35 μm from the interface were obtained from EDS counts at point 1, Figure 3. There is no meaningful difference in atomic ratios between the slag bulk phase and at interface for all elements except that for manganese. In the vicinity of the slag-metal interface, manganese concentration is visibly less than in the bulk slag phase, what can be explained by predominant MnO reduction from the slag. Concentration gradient of manganese in the slag indicates that manganese transfer in the slag can be a rate limiting stage in the MnO reduction.

3.3 Manganese and Silicon Partitioning between Slag and Metal Phases

The overall reduction of MnO from slag by carbon of a substrate can be represented by the reaction:

$$\text{MnO (in slag)} + \text{C (solid)} = \text{Mn (in alloy)} + \text{CO} \quad (1)$$

Relationship between the CO partial pressure and MnO activity in the slag can be obtained from the equilibrium constant for reaction (1):

$$K_1 = \left(\frac{a_{\text{Mn}} P_{\text{CO}}}{a_{\text{MnO}} a_{\text{C}}} \right)_{EQ} \quad (2)$$

Where

K_1 is equilibrium constant for reaction (1)
a_{Mn} is activity of manganese in metal
P_{CO} is CO pressure in gas, atm
a_{MnO} is activity of MnO in slag
a_{C} is activity of carbon of substrate

The equilibrium constant was obtained from the standard Gibbs free energy change for reaction (1) from [14]. Calculated P_{CO} *vs* a_{MnO} at 1450, 1550 and 1650 °C is plotted in Figure 4. In this calculation, activity of manganese in the Mn-C(sat) alloy was 0.4 [15], activity of carbon was equal 1. For nucleation and growth of the CO gas bubble at the substrate-slag interface, CO partial pressure should be at least 1 atm; corresponding equilibrium MnO activity in the slag to be 0.244 at 1450 °C, 0.081 at 1550 °C and 0.030 at 1650 °C. Activities of MnO in synthetic and industrial slags examined in this work were estimated using FACTSage (version 6 with a database developed by Tang and Olsen [13]) and are presented in Table 3. At experimental temperature of 1450 °C, activity of MnO in all slags but slag D was below the equilibrium value 0.244; while at 1550 °C, activity of MnO in slags A, D and E was above and in slags B, C and F below the equilibrium value 0.081. Run 14 showed that MnO was not reduced at 1450 °C, what confirmed results of thermodynamic assessment. MnO activity in the slag in this run was 0.131 which was below the equilibrium MnO activity of 0.244 at 1450 °C.

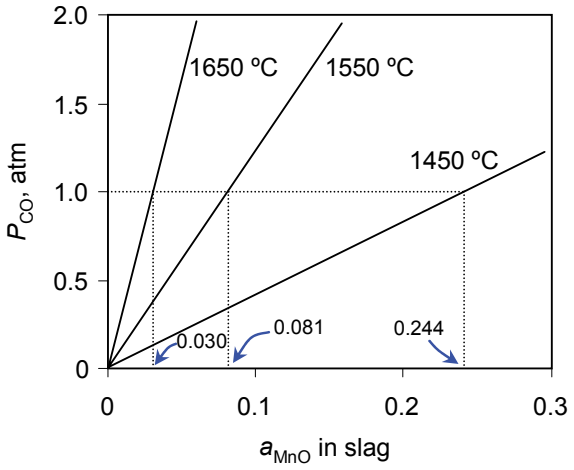

Figure 4: P_{CO} in equilibrium with MnO in slag.

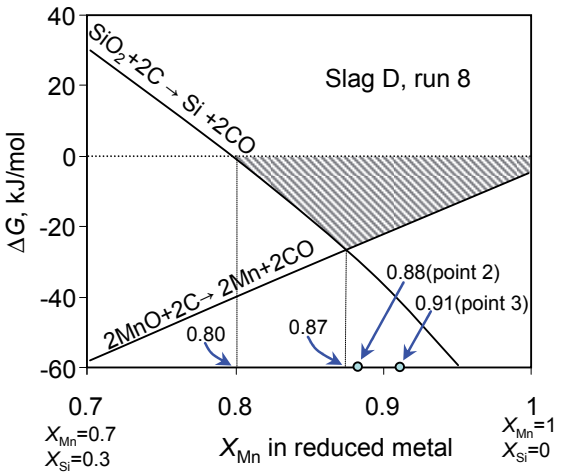

Figure 5: Gibbs free energy changes at 1550 ℃.

In cases when reduction of MnO from the slag to Mn-C alloy is not expected at the slag-substrate interface, there is a thermodynamic condition for its formation at the slag-gas-substrate boundary of slag perimeter as CO partial pressure in the furnace gas is about 0.004 atm according to the off gas analysis in the course of experiments. The reduction of MnO might occur *via* combination of cathodic reaction at the slag-carbon interface to produce a metal phase as seen in Figure 3 and anodic reaction at the slag perimeter to release CO.

Thermodynamic analysis shows that silica can be reduced simultaneously with manganese oxide to the Mn-Si alloy. The Gibbs free energy changes for MnO and SiO_2 reduction to the Mn-Si alloy as a function of the alloy composition are shown in Figure 5 for slag D (run 8) at 1550 °C. Standard Gibbs free energy changes for reactions of SiO_2 and MnO reduction were taken from [14], activities of MnO and SiO_2 in the slag were estimated using FACTSage, CO partial pressure was 1 atm and carbon activity was assumed 1. The activity coefficients in the Mn-Si alloy were taken from [16]. The Gibbs free energy plots indicate that the independent reduction of SiO_2 by carbon to pure metallic Si is not expected at the slag-carbon interface, however SiO_2 and MnO can be reduced simultaneously to the Mn-Si alloy of composition within shadowed area, i.e., X_{Mn}>0.80. No production of the alloy with X_{Mn}<0.80 is thermodynamically feasible as the Gibbs free energy change of silica reduction is positive. Actual composition of the Mn-Si alloy depends on the rates of MnO and SiO_2 reductions.

The equilibrium partitioning of silicon and manganese between slag and metal phases can be represented by

$$SiO_2 \text{ (in slag)} + 2Mn \text{ (in alloy)} = Si \text{ (in alloy)} + 2MnO \text{(in slag)} \quad (3)$$

Figure 5 indicates that X_{Mn} would be 0.87 if the equilibrium of reaction (3) was established at the slag-metal interface. Experimental manganese mole fraction in metal (normalized as Mn-Si binary alloy) in run 8 varied from 0.88 at point 2 to 0.91 at point 3 in Figure 3.

Lower manganese and higher silicon content at the slag-metal interface (point 2) than in the metal phase (point 3) may be explained by two possible mechanisms. The first one is that silica is reduced by metallic manganese at the metal-slag interface through reaction (3) what creates Mn and Si concentration gradients in the metal phase. Experimentally observed X_{Mn}=0.88 at point 2 at the slag-metal interface is reasonably close to equilibrium X_{Mn}=0.87 in accordance with reaction (3). The second mechanism suggests the simultaneous MnO and SiO_2 reduction at the slag-carbon interface to metallic alloy. The reduction of MnO is much faster than that of SiO_2 in the beginning of the reduction reaction what produces an alloy with high Mn concentration. Then MnO reduction slows down due the depletion of MnO in the slag close to the interface as indicated in Table 4. This changes in the relative reduction rates of MnO and SiO_2 may produce metallic phase of lower X_{Mn}.

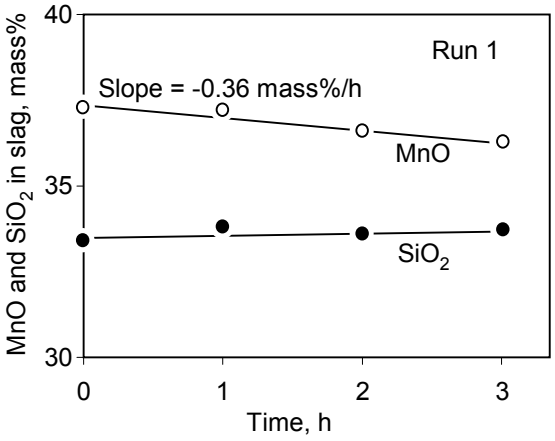

Figure 6: Variation of MnO and SiO_2 content in slag with time for run 1.

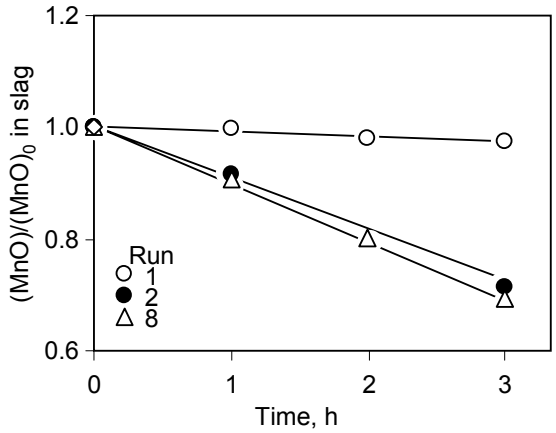

Figure 7: Variation of $(MnO)/(MnO)_0$ in slag with contacting time.

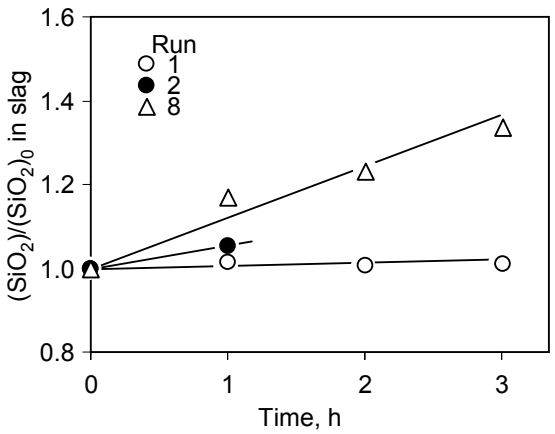

Figure 8: Variation of $(SiO_2)/(SiO_2)_0$ in slag with contacting time.

3.4 Slag Bulk Composition

Change in the chemical composition of slag as a result of reaction with carbon substrate was determined by XRF analysis. MnO and SiO_2 concentrations in the synthetic slag A in the progress of reaction with graphite substrate at 1550 °C (run 1) are shown in Figure 6. MnO content decreased as a result of reduction, while although silica was also reduced, SiO_2 content in slag slightly increased as reduction of MnO from the slag had a stronger effect on the slag chemistry than reduction of silica. This trend was more obvious in experiments, in which coke or/and industrial slag was involved. The variations of $(MnO)/(MnO)_0$ and $(SiO_2)/(SiO_2)_0$ in slag with reaction time in runs 1, 2 and 8 are shown in Figures 7 and 8, respectively. $(MnO)_0$ and $(SiO_2)_0$ are MnO and SiO_2 contents in the slag before reaction. Increase in SiO_2 was found to be higher than that estimated from the mass balance based on the amount of MnO removed from slag, particularly for those runs where coke substrate was used. This indicates that some SiO_2 in ash may dissolve into the slag phase *via* the slag-substrate interface. The weight ratio of ash to carbon in coke was about 1:9. When carbon at the surface of the substrate was partially consumed by reaction with oxides, the ash in the reacted carbon layer could dissolve into slag. The major component in the ash was SiO_2 (Table 2).

3.5 Rate of MnO Reduction

The reduction rate of MnO can be approximated by the slope of MnO concentration line as exampled in Figure 6 for run 1. The experimental reduction rate of MnO is shown in Table 3. Results can be summarized as: (1) reduction of MnO from the slag at 1450 °C was below the detectable level. Increase in temperature to 1550 °C significantly accelerated the reduction; (2) the reduction rates were generally higher in runs with coke substrates or with industrial (multicomponent) slags than in experiments with graphite substrate and synthetic (quaternary) slags; (3) the reduction rate increased with increasing MnO content in slag; and (4) the MnO reduction rate in experiment with graphite

substrate with higher surface roughness in run 13 was only slightly higher than that with lower surface roughness in run 1 under otherwise the same experimental conditions.

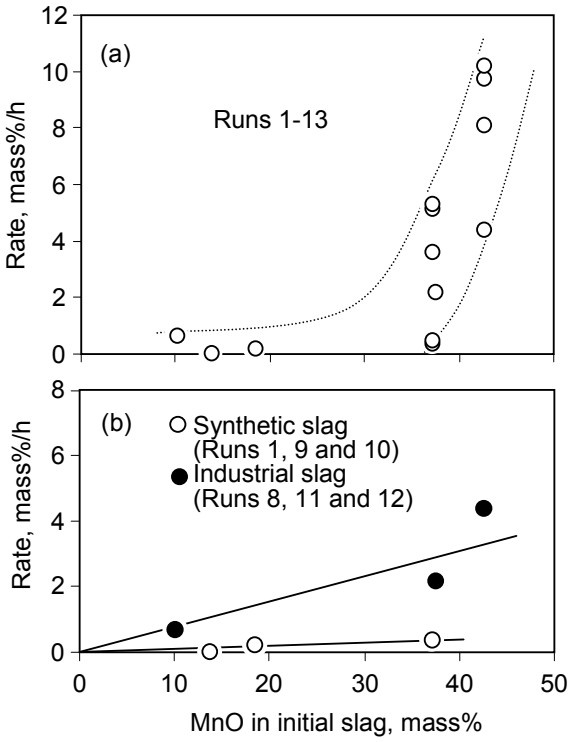

Figure 9: Reduction rate *vs.* MnO concentration in initial slag.

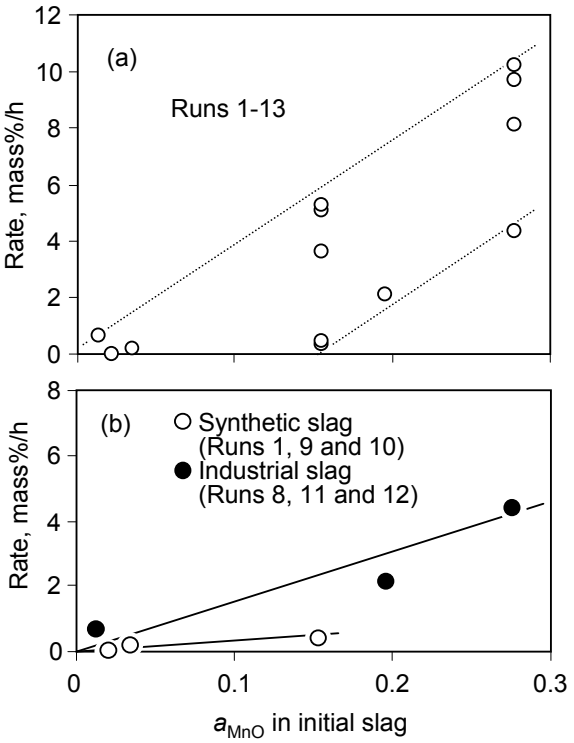

Figure 10: Reduction rate *vs.* MnO activity in initial slag.

The reduction rates at 1550 °C are plotted against MnO content and MnO activity in slag in Figures 9(a) and 10(a), respectively. The reduction rate was low for the MnO content in slag with up to 20 mass% but it increased sharply with increasing MnO content beyond 35 mass% (Figure 9(a)). A plot of the reduction rate against MnO activity is more close to linear, although experimental data are scattered (Figure 10(a)). Difference in the MnO reduction rate from synthetic and industrial slag is seen from plots of the reduction rate against MnO concentration in Figure 9(b) and MnO activity in Figure 10(b) for two groups of slags. The linear relationship between reduction rate and MnO concentration is an indication that the rate is chemically or mixed controlled by chemical reaction and mass transfer in the slag. The mixed control is supported by the EDS analysis in Table 4 which revealed the MnO concentration gradient in the slag. The minor components such as MgO, K_2O or Fe in industrial slags may be responsible for the difference in the reduction rate between two slag groups. Figure 11, which presents the rate of MnO reduction from slags A and D in reaction with graphite and coke substrates as a function of ash content, shows that the reduction rate increased with increasing ash content. This tendency is opposite to that observed for FeO reduction from the slag [17,18].

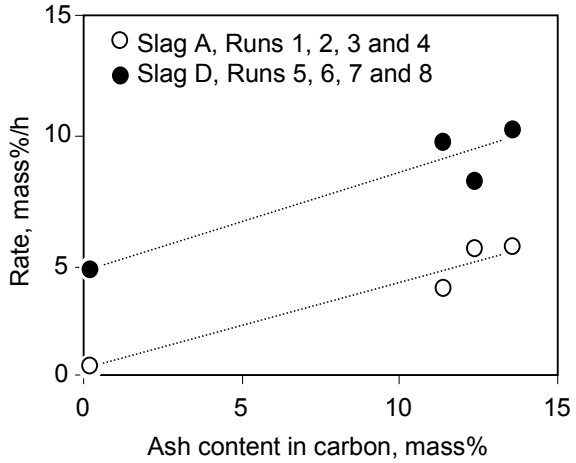

Figure 11: Reduction rate *vs.* ash content in carbon.

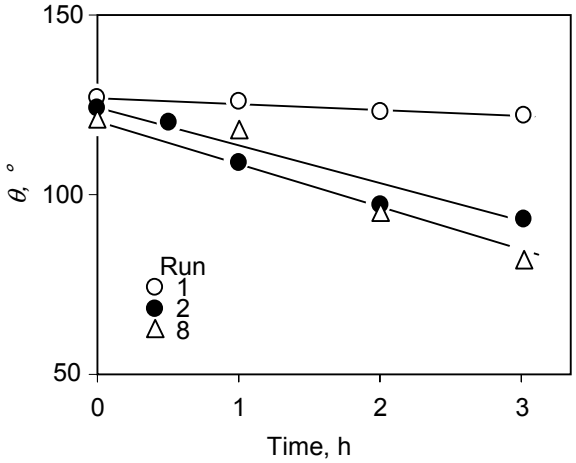

Figure 12: Variation of contact angle between slag and carbon with contacting time.

Surface roughness can affect CO bubble nucleation at the slag-carbon interface and, therefore, MnO reduction. In run 13, the graphite substrate had a rough surface in comparison with a polished substrate in run 1. The reduction rate of MnO on the graphite with rough surface was slightly higher than on polished graphite under otherwise the same conditions. A slight increase in the reduction rate with increasing carbon surface roughness was also observed by Safarian et al. [11] in experiments with similar slag but at higher temperature (1600°C). A small effect of surface roughness observed in work [11] and in this work indicates that its role in MnO reduction was not significant.

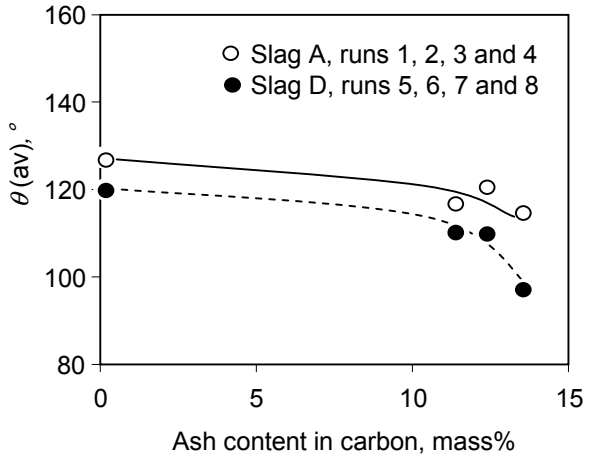

Figure 13: Contact angle *vs.* ash content in substrate.

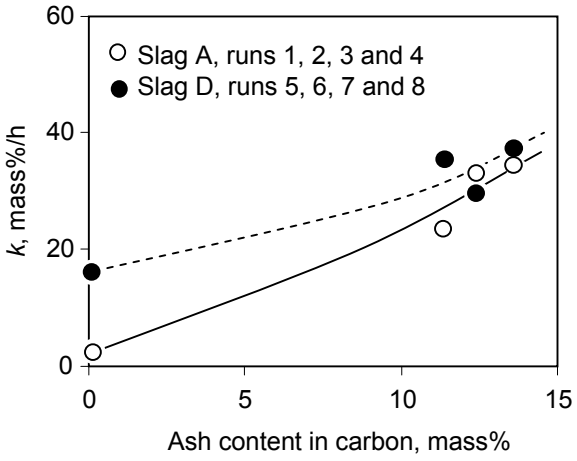

Figure 14: Apparent reduction rate constant *vs.* ash content in carbon.

3.6 Contact Angle

It is known that wettability of carbonaceous materials by slags is generally poor. The contact angles between slags and carbon substrates in runs 1, 2 and 8 are shown in Figure 12. The initial contact angle between slag A and graphite in run 1 was 127°; it decreased to 122° after 180 min contacting. The decrease in the contact angle was more profound in experiments with coke substrates (runs 2 and 8) than with graphite substrate (run 1). Ash of coke which was left behind at the slag-carbon interface after carbon was consumed by reaction with slag modified the slag-substrate interface and improved wettability, decreasing the contact angle. The wetting of graphite by the industrial slag in run 2 was also more dynamic than the wetting of graphite by the synthetic slag in run 1 (Figure 12). The average contact angle during 1 hour reaction is presented in Table 3. Results of the contact angle measurement can be summarized as: (1).the contact angle was slightly higher in runs with graphite substrates or synthetic slags than that measured in experiments with coke substrates and industrial slags; (2) the difference in the contact angle for the substrate with rough surface in run 13 and that with polished surface in run 1 was within the experimental error; and (3) the contact angle at 1450 °C in run 14 was close to that at 1550 °C in run 1. The contact angle was plotted in Figure 13

for synthetic slag A and industrial slag D in contact with graphite and coke substrates as a function of ash content in carbonaceous materials. The contact angle was found to decrease with increasing ash content.

3.7 Apparent Rate Constant

The linear relationship between reduction rate and activity of MnO in slag shown in Figure 10(b) indicates that the reduction of MnO in slag by carbonaceous materials is of a first order. This relationship was used to find the apparent rate constant, which is presented in Table 3. The apparent rate constant relates the reduction rate per unit MnO concentration or activity, what is useful for analysis of effects of other parameters rather than MnO concentration. Rate constants obtained in runs with coke and industrial slags were generally higher than those in experiments with graphite substrates and synthetic slags. As expected, it increased with temperature. Rate constant in experiment with substrate's rough surface was also higher than in run with the polished surface.

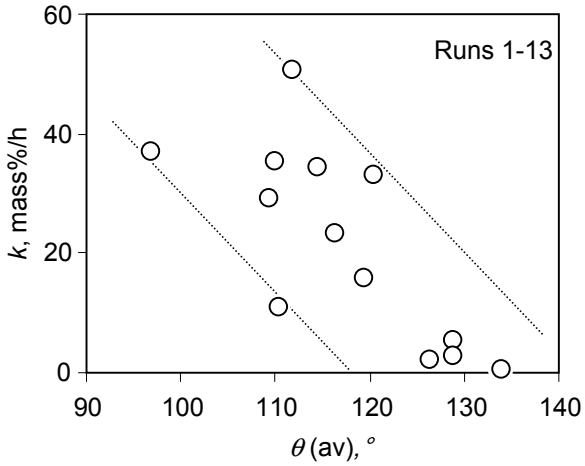

Figure 15: Apparent reduction rate constant *vs.* contact angle between slag and carbon.

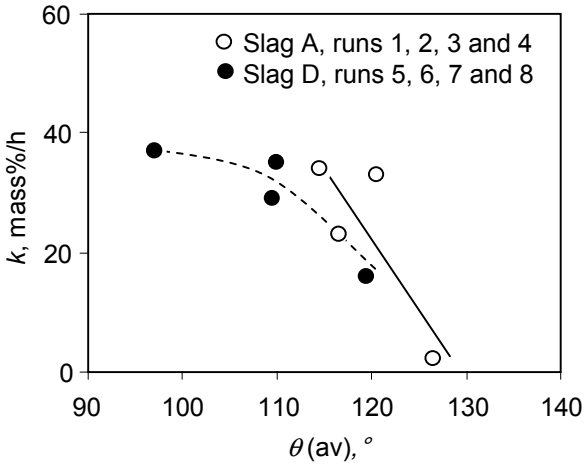

Figure 16: Apparent reduction rate constant *vs* contact angle between slags A and B and coke substrates with different ash content.

The effect of ash content in substrate on the reduction rate constant is shown in Figure 14 for slags A and D. The rate constant tends to increase with increasing ash content. Ash in carbonaceous materials may has twofold effect on the reduction rate constant, (1) catalytic effect of ash components, and (2) affecting the wettability between slag and carbon, which, in turn, may affect the reduction rate. The apparent reduction rate constants obtained in runs at 1550 °C are plotted against average contact angles in Figure 15. The apparent reduction rate constant decreased with increasing the contact angle. This tendency is more clearly shown in Figure 16 in which the rate constant is plotted against the contact angle for synthetic slag A and industrial slag D. The contact angle, and therefore the wettability, may affect the kinetics of MnO reduction through the interfacial area for elementary reactions involved in MnO reduction.

4 CONCLUSIONS

Wettability of graphite and coke by MnO-containing synthetic and industrial slags and MnO reduction were investigated at 1450 - 1550 °C. Reduced metal drops were observed at the slag-substrate interface and at the gas-slag-substrate boundary of slag perimeter. Carbon and silicon were dissolved in the reduced alloy. The MnO reduction rate increased with increasing MnO content in slag, temperature and ash content in the coke. Reduction of MnO was faster from the industrial slag than from the synthetic slag; it was also faster in reaction with coke substrate than with graphite. The contact angle between the slag droplet and substrate was slightly higher in runs with graphite substrates or synthetic slags than that measured in experiments with coke substrates and industrial slags. A correlation between MnO reduction rate and the contact angle was observed, which showed a tendency for the reduction rate to increase with decreasing contact angle or better wettability. The MnO reduction was found to be a first order reaction with regard to MnO activity in slag. Silica was reduced from the slag simultaneously with manganese oxide; manganese/silicon partitioning between metal and slag phases was close to equilibrium. Manganese oxide concentration gradient in

the slag was interpreted as an indication that MnO mass transfer in the slag was a contributing factor to the rate control.

5 ACKNOWLEDGEMENTS

This research was supported under Australian Research Council's Linkage Projects funding scheme (project number LP0560703).

6 REFERENCES

[1] Berg, K.L., SINTEF, 2001, Report No. STF24 A01637.
[2] Rankin, W. J., and Van Deventer, J. S. J. “The Kinetics of Reduction of Manganese Oxide by Graphite”, J. S. Afr. Inst. Min. Metall., 80(1980), 239-247.
[3] Rankin, W. J.,and Wynnyckyj, J. R. “Kinetics of Reduction of MnO in Powder Mixtures with Carbon”, Metallurgical and Materials Trans. B, 28B (1997), 307-319.
[4] Ostrovski, O. and Webb, T. “Reduction of Siliceous Manganese Ore by Graphite”, ISIJ Int., 35 (1995), 1331-1339.
[5] Lone, M., Sun, H., Ganguly, S. and Ostrovski, O. "Interfacial Phenomena and Reaction Kinetics between Carbon and Slag Containing MnO”, Proceedings INFACON XI 2007 Congress, New Delhi, INDIA, 18 - 21 Feb 2007, 594-613.
[6] Ostrovski, O., Olsen, S. E., Tangstad, M. and Yastreboff, M. M. “Kinetic Modelling of MnO Reduction from Manganese Ore”, Canadian Metall. Q., 41 (2002), 309-318.
[7] Yastreboff, M., Ostrovski, O. and Ganguly, S. “Effect of Gas Composition on the Carbothermic Reduction of Manganese Oxide”, ISIJ Int., 43 (2003), 161-165.
[8] Shibata, E., Sun, H. and Mori, K. “Kinetics of Reactions between MnO Based Slag and Fe-C-P-Si-S Alloy”, Tetsu-to-hagane, 82 (1996), 575-580.
[9] Shibata, E., Sun, H. and Mori, K. “Kinetics of Simultaneous Reaction between Liquid Iron-Carbon Alloys and Slags Containing MnO”, Metallurgical and Materials Trans. B, 30B (1999), 279-286.
[10] Safarian, J., Tranell, G., Kolbeinsen, L., Tangstad, M., Gaal, S., and Kaczorowski, J. “Reduction Kinetics of MnO from High-Carbon Ferromanganese Slags by Carbonaceous Materials in Ar and CO Atmospheres”, Metallurgical and Materials Trans. B, 39B (2008), 702-712.
[11] Siddiqi, N., Bhoi, B., Paramguru, R. K., Sahajwalla, V. and Ostrovski, O. “Slag–Graphite Wettability and Reaction Kinetics. Part 1 Kinetics and Mechanism of Molten FeO Reduction Reaction”, Ironmaking & Steelmaking, 27 (2000), 367-372.
[12] Siddiqi, N., Bhoi, B., Paramguru, R. K., Sahajwalla, V. and Ostrovski, O., “Slag–Graphite Wettability and Reaction Kinetics. Part 2 Wettability Influenced by Reduction Kinetics”, Ironmaking & Steelmaking, 27 (2000), 437-441.
[13] Tang, K., Olsen, S.E., “Computer Simulation of Equilibrium Relations in Manganese Ferroalloy Production”, Metallurgical and Materials Transactions B, 37B (2006), 599-606.
[14] Iron and Steel Handbook, I, “Fundamental Theory of Iron and Steel”, 3rd Ed., ISIJ, ed. Maruzen, Tokyo, 1981.
[15] Olsen S., Tangstad M., Lindstad T. “Production of Manganese Ferroalloys”, Tapir Academic Press, Trondheim, Norway, 2007.
[16] Ahmad, N. and Pratt, J. N. “Thermodynamic Properties of Liquid Manganese-Silicon Alloys”, Metallurgical Transactions A, 9A (1978), 1857-1863.
[17] Sun, H. and Easman, W. “Interfacial Phenomena and Reaction Kinetics between Carbon and Slag in Ironmaking Process”, Energy and Fuels, 21 (2007), 413-418.
[18] Sun, H. “Mathematical Modelling and Experimental Investigation of Coke Reduction of FeO in Slag”, Steel Research Int., 78 (2007), 659-666.